# Design and development of a high precision, high payload telescope dual drive system

Michael S. Worthington[a†], Timothy A. Beets[a], Joseph H. Beno[a], Jason R. Mock[a], Brian T. Murphy[a], Brian J. South[a], John M. Good[b]

[a]Center for Electromechanics, The University of Texas, 1 University Station R7000, Austin, TX, USA 78712;
[b]McDonald Observatory, The University of Texas, 1 University Station C1402, Austin, TX, USA 78712

## ABSTRACT

A high precision, dual drive system has been designed and developed for the Wide Field Upgrade to the Hobby-Eberly Telescope[*] at McDonald Observatory in support of the Hobby-Eberly Telescope Dark Energy Experiment[‡]. Analysis, design and controls details will be of interest to designers of large scale, high precision robotic motion devices. The drive system positions the 19,000 kg star tracker to a precision of less than 5 microns along its 4-meter travel. While positioning requirements remain essentially equal to the existing HET, tracker mass increases by a factor greater than 5. The 10.5-meter long tracker is driven at each end by planetary roller screws, each having two distinct drive sources dictated by the desired operation: one slowly rotates the screw when tracking celestial objects and the second rotates the nut for rapid displacements. Key results of the roller screw rotordynamics analysis are presented. A description of the complex bearing arrangement providing required degrees of freedom as well as the impact of a detailed Failure Modes and Effects Analysis addressing necessary safety systems is also presented. Finite element analysis results demonstrate how mechanical springs increase the telescope's natural frequency response by 22 percent. The critical analysis and resulting design is provided.

**Keywords:** Center for Electromechanics, Hobby-Eberly, HET, HETDEX, dual drive, precision motion control, tracking, robotic motion

## 1. INTRODUCTION

The Hobby-Eberly Telescope (HET), Figure 1, is located on Mt. Fowlkes in the Davis Mountain Range in West Texas and has been conducting science operations since October, 1999[1]. The HET support structure and primary mirror sits at a fixed zenith angle of 35º and can move in azimuth to access approximately 70% of the visible sky. The primary mirror, constructed of 91 identical hexagonal segments, forms an 11 m hexagonal-shaped spherical mirror with a 26,164 mm radius of curvature. The tracker mounts above the primary mirror on the upper-most portion of the telescope, termed the upper hexagon or "upper hex". The corrector optics mount to the tracker and are positioned via two linear drive systems and a six degree of freedom (DOF) hexapod maintaining the instruments' optical axis normal to and on the focal sphere of the primary mirror.

The Hobby-Eberly Telescope (HET) is currently undergoing a major redesign effort in preparation for the Wide Field Upgrade (WFU). The WFU involves replacing the current star tracker[2] along with its drive systems and corrector optics. The catalyst for replacing this hardware is to perform the Hobby-Eberly Telescope Dark Energy Experiment[3,4] (HETDEX). Replacing the current Spherical Aberration Corrector (SAC) with the Wide Field Corrector[5] (WFC) will increase the HET field of view from 4' to 22'. In addition, the current science instruments will be supplemented with the Visible Integral-field Replicable Unit Spectrograph[6] (VIRUS). These changes will allow the telescope to conduct the largest survey of distant galaxies ever attempted.

The primary impact to the WFU tracker caused by the replacement of the corrector optics is the approximately seven fold increase in mass of the instruments and supporting hardware. As a result, the WFU tracker mass increased on the order of 5 times that of the HET tracker. This increased load affects the majority of the component selection for the X-drive hardware, hence the necessity for replacing the existing equipment. The following sections focus on the X-drive system design, whose purpose is to position the corrector optics with a 5 micron precision anywhere along the X-axis' 4 meter travel. The X-drive, consisting of dual planetary roller screws each with two distinct drive sources, couples to the nearly 19,000 kg tracker and payload system which spans 10.5 meters across the upper hex. Detailed descriptions of the tracker bridge, Y-axis drive system, hexapod and controls development are provided in References 7-10 respectively.
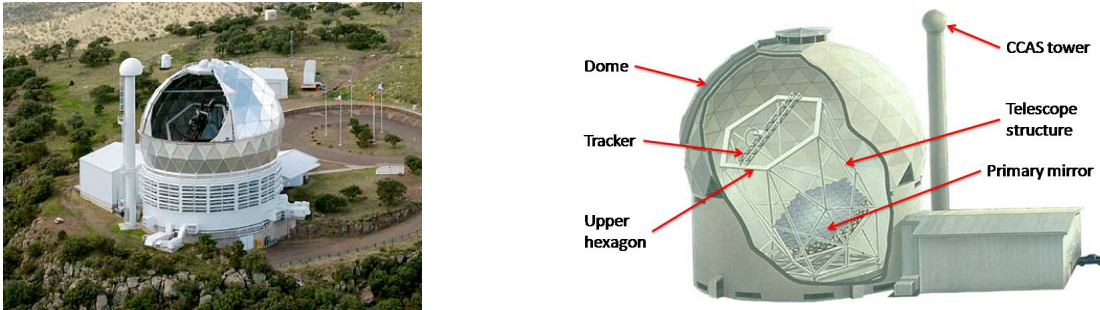


Figure 1. The figure on the left shows an aerial view of the HET with the shutter open. The computer rendering on the right reveals the major components of the telescope.

## 2. DRIVE SYSTEM

The HET has two primary linear axes, X and Y, as defined in Figure 2. The main structural component of the tracker is the bridge. The bridge traverses the upper hex along the X-axis and the corrector optics travel the length of the bridge in the Y-axis. The W-axis is the WFC optical axis which tips and tilts to remain on the spherical focal surface of the primary mirror at any location. The hexapod provides limited travel in the X, Y and W axes, along with rotations about each axis, theta, phi and rho respectively. When the tracker is centered over the primary mirror, the W and Z axes are coincident (X, Y and Z axes are orthogonal to each other).
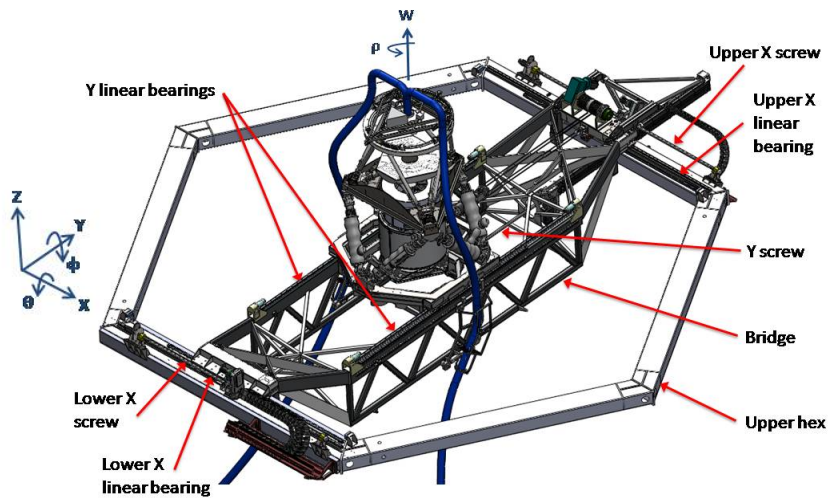


Figure 2. CAD model of the WFU tracker showing the key elements of the X and Y drive systems and the reference coordinate system

### 2.1 Linear bearings

Precision, profiled-rail linear bearings provide the primary DOF for the tracker. To distribute the large loads supported by these bearings, four bearing blocks are used on each rail compared to three blocks on the HET, in addition to increasing the bearing sizes. The linear bearings are manufactured by THK and utilize caged ball technology (SHS

series) to further increase load carrying capacity. To span the required 6045 mm distance, the bearing rails are manufactured from three separate rail sections with ground ends to ensure smooth transitions at the joints.

Due to the 35º mounting orientation of the tracker, the Lower-X (LX) bearing carries a greater load share. While the Z-axis component of the tracker's mass is essentially shared evenly between the bearings, the LX bearing reacts the entire Y-axis component. The bearing blocks react this load as both a side load and as a roll moment about the X-axis. The moment loading dominates the predicted life and static safety factor equations used to size the bearings. The increased load of the WFU tracker causes two problems: 1) the loads carried by the LX bearing reduce the theoretical life below the 20 year operational target and 2) the disproportionate load share decreases the telescope's first mode natural frequency from 4.5 Hz with the HET tracker to 4.39 Hz. Two measures are taken to solve these problems. The first involves integrating a spring pack, consisting of eight springs acting in parallel, between the Upper-X (UX) end of the tracker and the trolley, which in turn is mounted to the X-axis bearing blocks. The effective spring rate moves one-third of the Y-component weight onto the UX beam. Despite introducing a source of compliance to the overall system, structural Finite Element Analysis (FEA) of the entire telescope predicts the first mode increases to 5.12 Hz due to load sharing across the upper hex. To further increase the frequency response, two MC12x31 in. channels will be welded to either side of the LX beam of the upper hex to increase structural stiffness. Coupled with the spring pack, the first mode increases to an estimated 5.35 Hz.

FEA analysis is also used to estimate the deflection of the UX and LX beams under the weight of the new tracker. Due to the stiffness of the end sections of the bridge, concern exists about the loading condition of the four bearing blocks spanning the deformed rail. The outer two blocks are isolated while the middle blocks are connected via a "wobble plate" providing additional DOF to relieve these concerns. The wobble plate is discussed in additional detail in Section 3.

## 2.2 Planetary roller screws

As with the HET, the WFU tracker utilizes satellite roller screws to effect tracker movements along the X and Y axes. As shown in Figure 2, the X drive consists of a pair of rollers screws situated adjacent to respective linear bearings at the UX and LX beams. The pair of roller screws is driven in unison to move the bridge in the X direction. These rollers screws feature ground 60x10 threads (60 mm pitch diameter with 10 mm per turn lead) with a 6-start (6 satellite rollers) nut. The roller screws are manufactured by SKF and have considerable threaded lengths of 4515 mm. Both screws utilize zero-backlash preloaded nuts with end flanges to attach drive components. The Y-axis roller screw has several appreciable differences as discussed in Reference 11. Figure 3 illustrates the roller screw assembly prior to installation on the upper hex.



Figure 3. CAD illustration of the UX roller screw drive system (track drive motor and screw bearing mounts not shown).

Each of the X drive roller screws is coupled to dual drives, a track drive and a slew drive. The track drive is coupled directly to one end of the screw, referred to as the drive end, and rotates the screw. The slew drive is an offset belt drive that rotates the nut. The slew drive also includes components to couple the nut to the trolleys. This dual drive arrangement is essential to allow slow, precise tracking movements by directly turning the screw and faster slewing movements by rotating the nut. A single motor drive could not be identified which could effectively operate under this full range of conditions. Separating the functions allows each drive motor to be selected specifically for a more narrow operating window.

The X drive roller screws are supported by pillow block bearings on each end. The track drive ends are supported by an SKF pillow block (part number PLBU 63) which includes a pair of preloaded angular contact bearings. Opposite the track drive ends, the floating ends are supported by pairs of deep groove ball bearings within custom cylindrical bore housings. These housings include minimal radial clearance (between the housing bore and outer bearing races) to allow the bearings to shift axially, while eliminating radial play. The bearings are fixed axially to the screw with bearing retaining nuts. This fixed-floating (axially fixed at the drive end and axially floating at the opposite end) bearing

arrangement allows the screw to expand and contract due to thermal shifts and also prevents binding as the nut approaches the floating end.

Bearing mounts, shown in Figure 4, are rigidly attached to the respective upper and lower X beams and support the screw bearing blocks. (The track drive end bearing mounts also include features to mount the track drive components.) Each bearing mount is adjustable in all degrees of freedom allowing precise bearing alignment to the screw. The slew drive mounts are also adjustable to allow precise alignment of the nuts relative to the screws. The combined adjustability of the bearing and slew drive mounts is utilized to accurately align the screw axes to the tracker's path of motion.
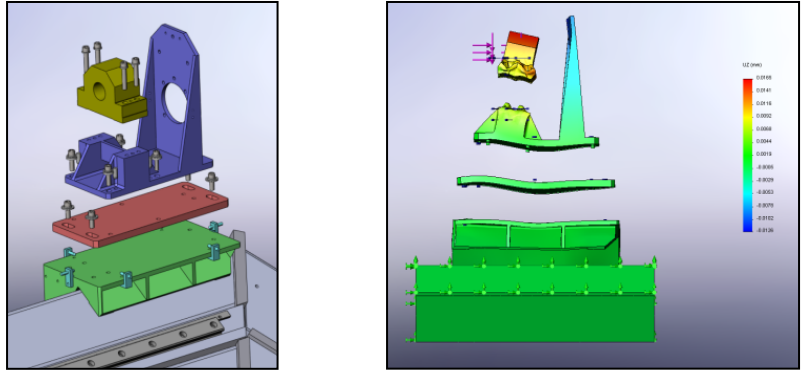


Figure 4. CAD exploded view of the screw drive end bearing block and mount and an exploded FEA model analysis.

As previously mentioned, the X drive has two primary operational modes: slewing and tracking. Operational parameters of the X-drive are shown in Table 1. Tracking and slewing are performed by dedicated, distinct drive systems. The track drive consists of a Kollmorgen AKM53G motor coupled to the drive end of the screw via a torque limiting shaft coupling (R+W model BK2-SK3-150). The couplings permit minor misalignment between the motors and screws. This model of torque limiter contains a ring that displaces axially when the set torque is overcome. The limiter then slips one full revolution and will re-engage if torque reduces below the set point. A proximity probe mounted to the drive mount monitors the ring on the limiter and signals the control system if this ring is moved by an over-torque situation.

Table 1. Operational parameters and capabilities of the X drive.

| | Linear Speed mm/s | Acceleration mm/s$^2$ | Mean Load kN | Load Applied kN | Peak kN (Motor) |
|---|---|---|---|---|---|
| Nominal Track Operation | $\leq 3$ | $\leq 0.5$ | 2.30 | 2.31 | N/A |
| Max Track Operation | 3 | 0.5 | 2.30 | 3.47 | 14.93 |
| Nominal Slew Operation | $\leq 80$ | $\leq 20$ | 2.30 | 9.71 | N/A |
| Max Slew Operation | 80 | 20 | 2.30 | 14.57 | 62.7 |

Each slew drive has an offset motor coupled to the nut with a belt drive, shown in Figure 5. This system is a substantial departure from the original HET design, but yields distinct advantages. Namely, the offset drive occupies less screw length, which reduces dead space on the threaded length. Additionally, the main components of the drive, the motor and gearhead, can be serviced without dismounting the screw. Each slew drive includes a Kollmorgen AKM53G motor, as is used on the track drives mounted to a 5:1 Danaher UT014 gearhead. The pulley diameter differential further adjusts the final drive ratio to 4.2:1. The driven pulley is bolted directly to the roller screw nut and the drive pulley is coupled to the gearhead output shaft via a torque limiter similar to that used on the track drive. This limiter (R+W model SK1 200) also has a ring that is displaced when the set torque is overcome. A proximity probe in the slew drive monitors the ring on the limiter and signals the control system if this ring is moved by an over-torque situation. The belt is a high-strength composite toothed timing belt from Gates, model 14MGT-1260-20.
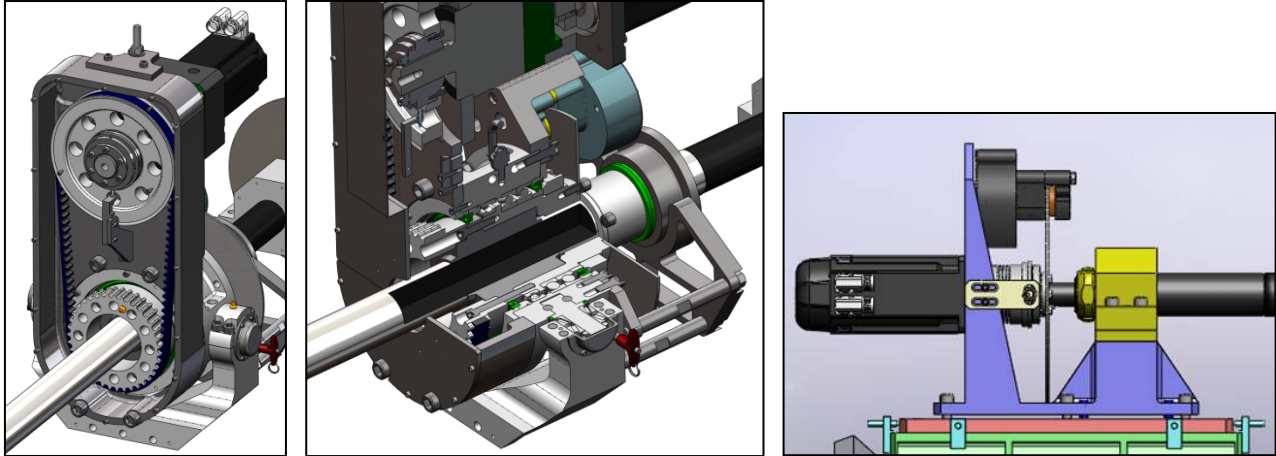
Figure 5. Detail views of X slew and track drives (far right image).

While either the track or slew drives is operating, the other drive is secured from rotation with a rotor and caliper type brake. The track drive rotors are attached to the torque limiter shaft couplings (refer to Figure 5), while the slew drive rotors are bolted to the nut carrier rotor. The track caliper is attached to the fixed end screw bearing mount, while the slew drive calipers are connected to the slew drive housing. The calipers are mounted on a floating mount that allows automatic compensation for pad wear and are spring biased to prevent pad-rotor drag. The calipers are spring-applied and pneumatically released. Accordingly, any power failure or pneumatic system failure will relieve sufficient air pressure causing all brakes to be applied, creating a fail-safe setup. The brakes may also be manually applied or automatically tripped (via software or hardware limits) in emergency situations. In emergency mode, applied braking torque is sufficient to slow and stop tracker motion from track or slew speed, while limiting deceleration loading of the tracker to reduce risk of damage to the corrector optics. Emergency-mode brake decelerations and displacements (including actuation time) are shown in Table 2. In normal operation, the brakes are not applied until the drive has come to a complete stop.

Table 2. Emergency-mode braking parameters.

| Operation | Velocity | Deceleration | Displacement |
|---|---|---|---|
| | [mm/s] | [mm/s$^2$] | [mm] |
| Track | 3 | 3924 (0.4 g) | 1.5 |
| Slew | 80 | 3924 (0.4 g) | 41 |

The X drive roller screws are essentially unsupported between the span of the fixed and floating bearings. The unsupported length (distance between bearings) is 4700 mm. As shown in Figure 6, the screws sag under their own weight due to the long length. Exhaustive analysis quantified the screw sag as 2 mm and highlighted that significant stresses are imparted on the satellite rollers in the screw nuts as the bridge nears end of travel at either bearing mount, as shown in Figure 7. The stress is especially high near the fixed bearing mount, shown at the left end of the screw in Figure 6. The roller screw imparts a radial load on the nut near the center of travel, but the load state shifts from radial to moment loading as the nut approaches the bearing blocks. Moment loading of the nut causes the satellite rollers to be asymmetrically loaded, causing stress concentrations, which can severely reduce screw and nut life.
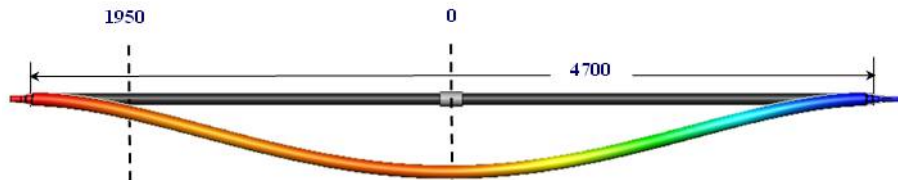


Figure 6. CAD illustration (exaggerated) showing calculated X drive screw sag of 2 mm maximum.
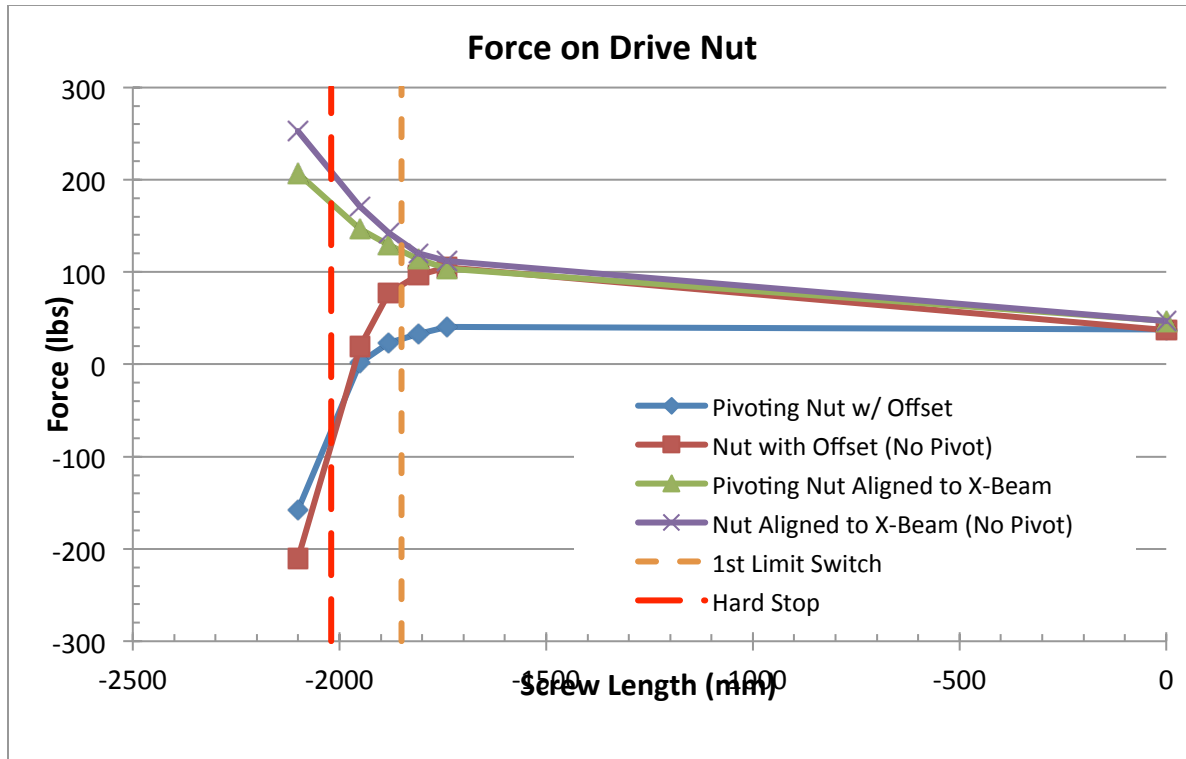
Figure 7. Graphical illustration of forces on roller screw nut increasing as nut travel nears screw ends (0 length is screw's midpoint).

Special considerations were made to the design of the X drive to minimize the stresses on the roller screw nuts. First, the support bearings at the fixed and floating ends of the screws are paired (duplex paired back-to-back angular contact bearings at the fixed end and paired deep groove ball bearings at the floating end) to better restrain the ends of the screws in straight and concentric orientations. Second, the screw nuts are positioned 0.43 mm below the straight-line screw axes. This offset reduces stress in the nuts for the full travel over the screw. Additionally, the slew drives are mounted on a pivot mechanism to provide a degree of rotational movement about the central transverse axis of the nut. As shown in Figure 5, the slew housings are equipped with horizontally extending trunnions, which are supported on bearings, referred to as the pivot bearings. The pivot bearings are retained within the slew drive yoke. The yoke forms the support that couples the slew drive to the bridge.

## 2.3 Rotordynamic analysis

Despite relatively slow rotational speeds of the screw/nut, the length of the screw caused concern of operating near a critical speed. A rotordynamics analysis was performed on the screw using XLRotor software with the goal of calculating the lateral modes of vibration of the screw as a function of nut position. The model includes the pivot nut design and provides appropriate stiffness values for the duplex ball bearings on each end, yoke bracket and satellite rollers within the nut. The slew drive assembly is represented by a concentrated mass with appropriate inertia properties, as is the brake disc and coupling.

The pivoted support of the nut drive mechanism causes asymmetric lateral vibration modes. This means there are different modes in the X-Y and X-Z planes. Figure 8 displays the results of the lowest four critical speed modes as a function of nut position. The first mode ranges from 879 rpm when the nut is centered to 500 rpm at the end of travel. Nut rotation corresponding to max slew speed is 480 rpm, which is within the desired 20% margin from critical speed at the ends of travel. Experimental tests will be conducted when the system is assembled to determine if the slew speed needs to be decreased near the ends of travel to prevent exciting a resonant frequency.
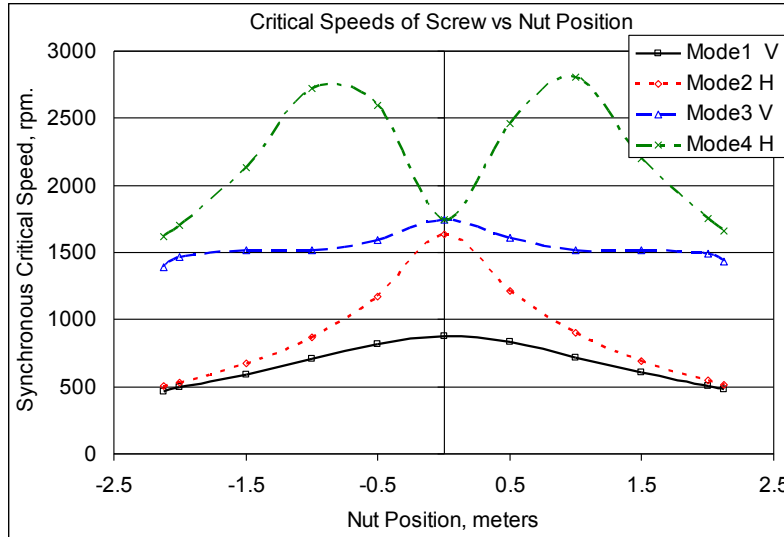
Figure 8. Mode frequencies as a function of nut position (V = vertical plane, X-Z; H = horizontal plane, X-Y).

## 3. SKEW SYSTEM

Inherent to the dual drive configuration, one end of the tracker can lead the other end resulting in a skew condition. To prevent the linear bearings from binding, additional DOF are introduced to the interface between the tracker bridge and linear bearings. Limit switches are also used to identify discrepancies between the two drives and limit relative displacement between tracker ends to 100 mm. A limit switch disables the high voltage contactors from the servo amplifiers and engages the screws' disc brakes if the 100 mm limit is reached.

Both ends of the tracker use three bearing sets to allow rotation relative to the upper hex. Mounted to the center of the tracker is a double-row spherical roller bearing termed the "skew bearing". In addition to being the central rotation point for the tracker, the skew bearing transmits the Y-axis loads from the tracker to the X-axis linear bearing. The skew bearing reacts a large radial load that is constant in direction and while rotation is required, it is limited to only 0.54 degrees during operation (a result of the 100 mm delta displacement). This limited rotation means that individual rollers within the skew bearings are constantly loaded, and the loads are not evenly distributed between rollers. Careful attention to the sizing and preloading of the bearing is taken to ensure successful performance for this application. The skew bearing is pressed onto a shaft mounted to a plate located between the bearing stacks and the bridge. A housing is then pressed onto the outer ring of the bearing which is bolted to the flexure plates.

Assisting the skew bearings are additional bearings at the corners of the tracker. For the HET tracker, plain bearings were used on the corners. While this prevented downward movement of the tracker, the corners are not constrained from lifting off of the trolley. As a result, the exact Z-axis load share between the two corners and the central skew bearing is not known. Given the greater deflection of the upper hex with the heavier WFU tracker, it is feared that the Z-loads across these three points could shift as the tracker travels the length of the X-axis, possibly resulting in lift-off. To more securely hold the bridge in place, THK HCR bearings are designated. The HCR bearings operate very similarly to linear bearings with the exception that the rails are curved. The bearing blocks therefore follow an arc-shaped path and are capable of sustaining loads in both the Z and -Z directions, as well as radial loads. Two HCR bearing blocks are used per corner to distribute the load to each rail. The HCR bearings are located above the outer X-axis bearing blocks and are positioned along the X-axis so that all three bearing sets share a common rotation point.

The wobble plate, Figure 9, ties the skew bearing to the two middle X-axis linear bearing blocks via kinematic ball mounts. The balls allow the individual blocks to conform to the deformed rail by rotating independently. The skew bearing also permits rotational DOF allowing the wobble plate to tip or tilt accordingly given the upper hex beam deflections in both the Y and Z axes. The Y-axis loads carried through the kinematic balls also prevents the blocks from experiencing a yaw moment, further decreasing the life expectancy. The balls are captured by bronze conical recesses mounted to the bearing blocks.
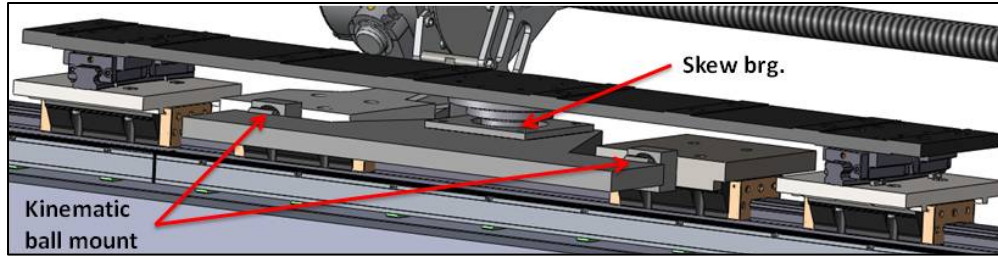
Figure 9. LX wobble plate prior to bridge installation illustrating the three mounting points.

## 3.1 Lower-X

Figure 10 shows the end view of the LX side of the tracker. Visible are the four X-axis blocks with the HCR bearings mounted directly above the outer two X-blocks. The skew bearing housing can be seen at the mid-span of the bridge. Magnitudes of loads carried in each axis for the bearings are displayed in Table 3. The dominating loads driving the safety factor and life equations can clearly be seen for each bearing. The arrows in Figure 10 represent the loads supported by each block in the following manner:

- Corner bearing stacks:
    - support vast majority of the Z-axis loads (blue arrows);
    - HCR bearings react relatively minor X-axis load from screw driving force (red arrows)
- Center bearing stack:
    - reacts Y-component of the tracker's weight (shown as yellow arrows coming out of the page)
    - supports small share of Z-load (essentially acts as a preload on the skew bearing)
    - skew bearing reacts driving force as a radial load while X-axis blocks react load as a pitch moment about Y-axis due to mounting location of nut
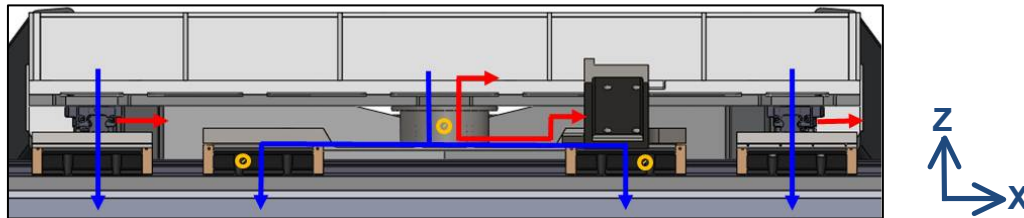


Figure 10. End view of the LX end of the bridge showing the bearing arrangement and load paths where blue lines represent Z-axis loads, red lines are X-axis loads and yellow lines (out of the page) are Y-axis loads.

Table 3. Loads (N) supported by each linear bearing block shown per axis and the summed total.

| Load | LX | | | | UX | | | |
| | Corner | | Trolley | Corner | | | Trolley | |
| | HCR45 | SHS65 | SHS65 | HCR45 | SHS45 | SHS55 | SHS45 | SHS55 |
|---|---|---|---|---|---|---|---|---|
| X-axis | 3000 | 0 | 0 | 3000 | 3000 | 0 | 3000 | 0 |
| Y-axis | 0 | 0 | 35,415 | 0 | 0 | 0 | 0 | 19,372 |
| Z-axis | 16,467 | 32,933 | 5000 | 16,467 | 32,933 | 32,933 | 5000 | 5000 |
| Equivalent load from moment | 0 | 0 | 58,399 | 0 | 0 | 0 | 15,840 | 21,355 |
| Total Load | 19,467 | 32,933 | 98,814 | 19,467 | 35,933 | 32,933 | 23,840 | 45,727 |

*HCR45 bearings have two blocks per corner - loads shown are per block

## 3.2 Upper-X

The UX end has a very similar bearing arrangement with the addition of one DOF in the Y-direction to prevent the bridge from binding in skew, Figure 11. The extra DOF is implemented with another set of linear bearing rails, the X-axis cross-slide bearings. Given the very limited rotation allowed in skew, only ±0.5 mm of travel in the Y-direction is

needed. The cross-slide bearings are therefore very short, providing 45 mm of travel for skew and to accommodate tolerance stack-ups during initial assembly.
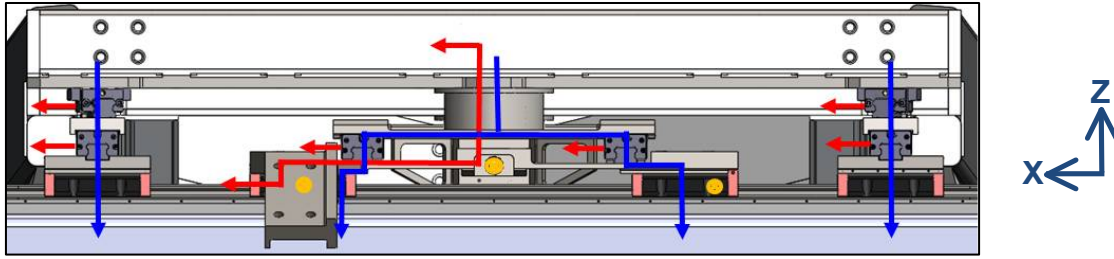


Figure 11. End view of the UX end of the bridge showing the bearing arrangement and load paths where blue lines represent Z-axis loads, red lines are X-axis loads and yellow lines (into the page) are Y-axis loads.

Four cross-slide bearings are utilized, two in the corners and two supporting the skew bearing in the center stack. On the corners of the bridge, the cross-slides are located between the X-blocks and the HCR bearings. These bearings are subject to the same loading as the other bearings in these stacks, dominated by the Z-component of the tracker weight and also includes the driving load from the screw.

The center bearing stack on the UX end includes one additional part: the spring mount plate, located just below the skew bearing. The purpose of the spring pack is to force load sharing between the UX and LX beams as described in section 2.1. This plate bolts to the skew bearing housing and the cross-slide blocks and acts as the flexure on the UX end to compensate for the deflecting upper hex beam. In addition, the spring pack mounts to the front section of this plate. A rod rigidly attached to the spring pack passes through a clearance hole in the spring mount plate and is threaded into the trolley, which in turn is bolted to the middle two X-blocks. The front section of the spring mount plate reacts the load being supported by the spring pack.

The loads on the center bearing stack are similar to the LX end. A small Z-component load is supported by the center stack, creating a roll moment on the center pair of cross-slide blocks. The cross-slide blocks and skew bearing transmit the driving force to the bridge which in turn drives the outer bearing stacks. The spring pack creates a force in the negative Y-direction which is reacted by the center X-blocks. These blocks transmit the load both as a side load and a roll moment. Magnitudes of the UX bearing loads are also shown in Table 4.

### 3.3 Anti-skew blocks

Early in the design phase, a detailed failure modes and effects analysis (FMEA) was performed on the tracker. The primary purpose of the FMEA is to identify potential failures that could result in significant safety and/or economic damages. Upon identifying potential failures modes, each is analyzed and assigned a numeric score in terms of severity, probability of occurring and likelihood of detection prior to failure. Of the 200 failure modes identified, 27 scored above the risk priority threshold meriting corrective action. Implementing the torque limiting couplings and the addition of the second mechanical limit switch at the ends of travel resulted from the FMEA.

The absolute worst-case failure identified during the FMEA involves the failure of several controls and limit switches resulting in the tracker separating from the upper hex and falling onto the primary mirror. The current HET mitigates this risk by looping a pair of large nylon straps around the UX beam of the upper hex and the bridge. In the event that the tracker separates from the upper hex, its fall would be limited to approximately one meter. While significant hardware would be damaged in this event, a recovery would be possible.

In lieu of allowing the WFU tracker to fall any distance, four large weldments, named the "anti-skew blocks", are welded onto the bridge with the intent of contacting the upper hex beams in severe skew conditions, Figure 12. The blocks significantly increase friction and will eventually wedge the tracker within the upper hex preventing further rotation. Adjustable pads bolt onto the weldments to provide the desired clearance during normal operation. Providing a 10 mm gap between the pads and upper hex allows the bridge to rotate 0.75° before contact. Another weldment is bolted onto the bottom sides of the anti-skew blocks. These tubes extend underneath the upper hex and will engage the bottom surface of the beams to prevent the tracker from lifting off of the upper hex. The gaps provided may be adjusted once the

tracker is installed to account for deflections in the upper hex beams in the Y and Z axes to ensure proper clearance exists throughout the travel. As the absolute last line of defense, the blocks are designed to withstand the worst-case loading scenario imaginable. This case would require the simultaneous failure of multiple layers of safety systems, both within software and hardware.
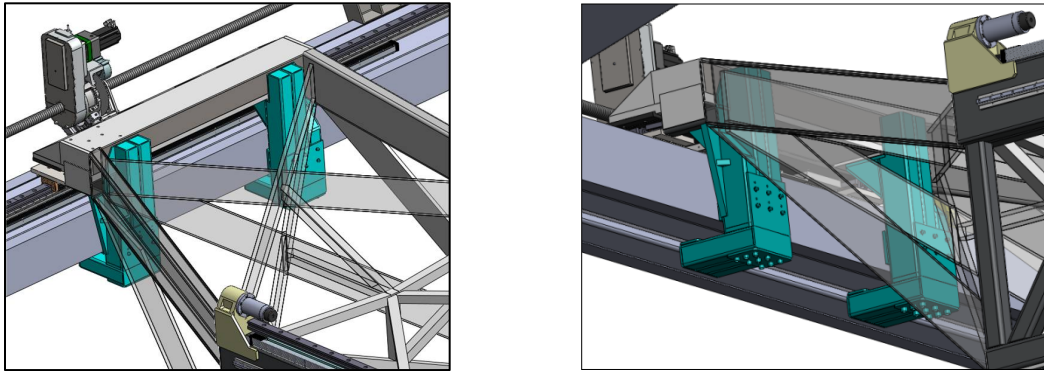


Figure 12. CAD model of LX end of bridge with anti-skew blocks (shown in blue) and bridge members semi-transparent

# 4. CONTROL ARCHITECTURE

## 4.1 Sensors

Controlling the X-drive system requires moving the upper and lower X-drives in concert. Independent linear sensors on each X-drive provide the primary feedback for the motion controller. Numerous secondary sensors are necessary for fault detection. The sensor suite for the X-drive system includes:

- (2) LB382 incremental encoders from Heidenhain Corporation. These sensors have a measuring length of 4440 meters, a grating period of 40 microns, and an accuracy grade of +/- 5 microns.
- (2) PT5DC string potentiometers from Celesco Transducer Products, Inc. These sensors have a measuring length of 5 meters and a resolution of 0.2 mm.
- (12) GLC limit switches from Honeywell, Inc. Redundant switches are installed at each end of each X rail. Additionally two limit switches are installed at the upper and lower X skew bearings.
- (4) AM1 proximity sensors from Automation Direct.
- (6) SA2F temperature sensors from Omega.

## 4.2 Start-up conditions

Due to the incremental nature of the LB382 sensors, the head unit must move roughly 25 mm on power-up to find a 'home' mark. During this time the controller has no absolute indication of the X position. This could result in running into end stops. Therefore, a secondary absolute sensor (the PT5DC) is selected to run in parallel. This coarse sensor allows the controller to know the X location within a reasonable precision. This information guides the controller to safely command the X system to find a 'home' mark for the LB382 sensors. Heidenhain does offer an absolute linear encoder that has the required travel capability for the X-axes, but the upper hex beams do not meet the required flatness and stiffness requirements for proper use. Therefore the two sensor approach is applied.

## 4.3 Travel limits

Each X-drive has two mechanical limit switches near the end of travel on each side. Tripping any individual switch will initiate an identical response to both drive systems, providing redundancy. In addition to the two mechanical limit switches, there is a software limit. These limits operate in sequence and have different purposes:

- Software Limit: Within the controller software, a travel limit is set to stop any motion once the X-drive exceeds this limit. This limit is based off of the feedback from the main LB382 sensors on the X rails.
- Limit Switch 1: When engaged by the X trolley, this sensor indicates to the control system that it has been reached and applies motor braking.

- Limit Switch 2: When engaged by the X trolley, this sensor indicates to the control system that it has been reached and it disables the high voltage contactors from the servo amplifiers and engages the screws' disc brakes.
- Bump Stops: Failure of the above safeties result in collision with hard stop cushioned with a urethane pad.

Table 4. Location and response parameters of limit switches at ends of travel

| Limit | Actuation | ±X Location | Deceleration Rate | |
|---|---|---|---|---|
| | | [mm] | [mm/s$^2$] | [gees] |
| Software | software | < 1850 | 20 | 0.002 |
| Limit switch 1 | software | 1850 | 300 | 0.03 |
| Limit switch 2 | software & hardware | 1880 | 3924 | 0.4 |
| Bump stops | hardware | 2020 | 4905 | 0.5 |

The trolley geometry is designed such that once a limit switch is engaged, it remains engaged even if the trolley impacts the hard stop. It can only be disengaged by reversing direction and exiting the limit switch position. The purpose of the sequential limit switches is to assure that no high speed collisions into bump stops are possible. Even if the controller software does not respond appropriately to the first limit switch, the second limit switch will stop the X-drive by disabling power and engaging the brakes.

## 4.4 Control algorithm

The X-drives are mechanically independent from each other and offer difficulties in creating smooth concerted motion. The UX and LX drives include differences in rail sag, roller screw accuracy, drive loads and friction. X-drive control software resides in the integrated tracker controller and consists of three fundamental elements:
- Independent trajectory control – Each X-drive has a motion controller which bases its feedback off the LB382 sensor. Using PID algorithms, the primary command for the drive is calculated. Additional algorithms are included for friction compensation, filtering and a feed-forward algorithm to accommodate constant loads, reduce gains and command magnitude for the PID commands.
- Relative skew control – The difference between the upper and lower LB382 sensors produces a skew error. Using separate PID algorithms, this error generates a supplementary command for each drive. The lagging drive receives a command to increase force while the leading drive is commanded to decrease force. The net force on the system remains the same and is dictated by the two independent controllers.
- Compensation tables – Minor corrections are automatically implemented to account for the inaccuracies in the rails, roller screws, and other mechanical components throughout the travel range.

Control algorithms are developed in the MATLAB-Simulink environment. Also in this environment, a complete tracker mechanical/dynamic model was developed that links to control Simulink models to allow exploration of impact from friction, sensor sensitivity and discretization, servo-amp characteristics, and sensor characteristics. The model allows advanced development of specialized control algorithms as necessary and initial tuning prior to hardware implementation. Simulink control modules are directly transferred to the tracker control system (dSpace hardware) via autocode generation without the need for writing basic C-level code.

## 4.5 Fault conditions

Fault monitoring is an important function for the X-drive controller. A fault causes the controller to stop X-drive motion and engages the brakes. Faults such as the 2$^{nd}$ travel limit switches and the skew limit switches will automatically disable the high voltage contactors and engage the X brakes. The various fault conditions monitored are:
- Over-travel – Both software and limit switches continually monitor for over-travel conditions.
- Over-torque – Torque limiting couplings are used to mate the drive motors to the drive screws. Proximity sensors monitor the state of these couplings. The sensor indicates to the control system when an over-torque condition has occurred and disables the high voltage contactors from the servo amplifiers and engages the X brakes.
- Over-current – Software continually monitors motor current. Due to the repetitive nature of the X-drive motion, the current required is well defined. If the motor current exceeds a specified value then a fault is generated.

- Skew – Both software and skew limit switches continually monitor for excessive skew conditions.
- Over-temperature – Temperature sensors mounted on the motor housings are used to detect over-temperature conditions.
- Linear Sensors – The PT5DC absolute sensors are continually compared to the LB382 sensors. A fault is generated if the indicated position from the two sensors is not the same within a certain tolerance.

## 5. SUMMARY

Design of a dual drive system for a high precision telescope is nearing completion with major components on order. Use of twin roller screws to drive the 10.5-meter, 19,000 kg tracker is similar to the current HET design with key differences. While the dual drive system approach is maintained, i.e. separate drive motors for tracking and slewing, the offset configuration implemented on the slew drive provides several advantages: improved maintenance accessibility, less dead space on threaded length allowing use of a shorter screw and provides a modular assembly preventing the need to remove the nut from the screw. The addition of the pivot nut design and DOF on the screw bearing housings allow the screw to be aligned in a manner which reduces radial loads on the nut at the extreme ends of travel. Key safety additions include the use of additional limit switches at the ends of travel, torque limiters on all drive motors to prevent over-torque and runaway scenarios and anti-skew blocks preventing separation of the tracker from the upper hex. Implementing THK arced linear bearings in place of plain bearings on the corners of the bridge will create superior joints ensuring more uniform load sharing across the X-axis linear bearing blocks.

## ACKNOWLEDGMENT

## REFERENCES

[1] Ramsey, L.W., et al., "The early performance and present status of the Hobby-Eberly Telescope," Proc. SPIE 3352, 34-42 (1998)

[2] Booth, J. A., Ray, F. B., and Porter, D. S., "Development of a star tracker for the Hobby Eberly Telescope," Proc. SPIE 3351, 298-309 (1998)

[3] Hill, G. J., et al., "The Hobby-Eberly Telescope Dark Energy Experiment (HETDEX): Description and Early Pilot Survey Results," ASP Conf. Series, 115-118 (2008)

[4] Savage, R.D., et al., "Current status of the Hobby-Eberly Telescope wide-field upgrade," Proc. SPIE 7733-149 (2010)

[5] Burge, J. H. et al, "Development of a wide-field spherical aberration corrector for the Hobby-Eberly Telescope," Proc. SPIE 7733-51 (2010)

[6] Hill, G. J., et al., "VIRUS: a massively replicated 33k fiber integral field spectrograph for the upgraded Hobby-Eberly Telescope," Proc. SPIE 7735-21 (2010)

[7] Worthington, M. S., Nichols, S. P., Good, J. M., Zierer, J. J., Mollison, N. T., Soukup, I. M., "Design and analysis of the tracker bridge for the Hobby-Eberly Telescope wide field upgrade," Proc. SPIE 7733-147 (2010)

[8] Mollison, N. T., Mock, J. R. Soukup, I. M., Beets, T. A., Good, J. M., Beno, J. H., Kriel, H. J., Hinze, S. E., Wardell, D. R., "Design and development of a long-travel positioning actuator and tandem constant force actuator safety system for the Hobby-Eberly Telescope wide-field upgrade," Proc. SPIE 7733-150 (2010)

[9] Zierer, J. Z., Mock, J. R., Beno, J. H., Lazzarini, P. G., Fumi, P., Anaclerio, V., Good, J. M., "The development of high-precision hexapod actuators for the Hobby-Eberly Telescope Wide Field Upgrade," Proc. SPIE 7733-49 (2010)

[10] Mock, J. R., Beno, J. H., Zierer, J. J., Rafferty, T. H., Cornell, M. E., "Tracker controls development and control architecture for the Hobby-Eberly Telescope dark energy experiment," Proc. SPIE 7733-152 (2010)